Materials Characterization 150 (2019) 62–66

Contents lists available at ScienceDirect

Materials Characterization

journal homepage: www.elsevier.com/locate/matchar

Effects of interface area density and solid solution on the microhardness of Cu-Nb microcomposite wires

Liping Deng[a,*], Zhifeng Liu[a], Bingshu Wang[b], Ke Han[c], Hongliang Xiang[a,*]

[a] School of Mechanical Engineering and Automation, Fuzhou University, Fuzhou 350116, China
[b] College of Materials Science and Engineering, Fuzhou University, Fuzhou 350116, China
[c] National High Magnetic Field Laboratory, Tallahassee, FL 32310, USA

ARTICLE INFO

Keywords:
Cu-Nb microcomposite wires
Interface
Solid solution
Microhardness

ABSTRACT

Cu-Nb microcomposite wires drawn to different strain values were studied by means of scanning electron microscopy and transmission electron microscopy. The Cu and Nb near the interfaces show a typical Kurdjumov-Sachs relationship with a deviation angle of 12°. This deviation accommodates internal stresses and slip discontinuity between Cu and Nb. The dislocations are mainly stored around the interface near the Cu matrix. Lattice distortion occurred near the interfaces, where Nb is believed to mix into Cu matrix. Microhardness is affected by interface area density as well as by strain-induced lattice distortion, which can produce a supersaturated solid solution.

1. Introduction

Cu alloys and composites with high electrical conductivity and high mechanical strength have shown wide promise in many fields [1–4]. The Cu-Nb composite is a special system which shows a good combination of high electrical, high thermal conductivity and high strength as well as limited grain growth at high temperatures [5,6]. These characters allow the composites to be applied in many fields, such as defense and military, magnets building and aerospace industry. The accumulative drawing and bundling (ADB) process [3,7], which has been proposed for decades and can subjected to more strain, introduces a more linear, continuous and uniform distribution of Nb ribbons, and correspondingly a higher conductivity and strength as compared to those in in situ Cu-Nb composite wires. Either in the in situ wires or non-in situ wires, the interface has been proved to be of great importance on the properties including mechanical, electrical and magnetic properties [1,8–11]. The high interface area density obtained after severe plastic deformation leads to enormous hardening far beyond the values estimated by Hall-Petch relationship, and the effect of the interface area density on the hardness has been given quantitatively [5,12].

Based on the Cu-Nb binary phase diagram, the mutual solubility between Cu and Nb is negligible (< 0.1 at.%) [13,14]. This should be true not only for in situ wires, but also for ADB wires. However, for mechanical alloyed Cu-Nb, which can be treated as in situ composites, ball milling process has been proved to allow immiscible elements to form supersaturated solid solution. The solid solubility can be up to 10 at.% Nb dissolved into the Cu matrix, inducing strengthening to the composites [15–17]. Kapoor et al. reported that Nb solid content can contribute up to 50% of the strength in mechanical alloyed Cu-Nb [18], where lattice distortion can be observed due to the differences in the radii of component atoms [12,19]. Jia et al. [20–23] stated that the strength of Cu-Nb composite wires is mainly related to the sizes of the phases, the grain orientation and the Cu-Nb interface structure. The limited solid solution was mainly found to occur around the Cu-Nb interfaces and has not been observed obviously or widely in these non-in situ Cu-Nb systems. For Cu-Nb composites fabricated by processes other than mechanical alloying, such as accumulative drawing/rolling and bundling (ADB/ARB) Cu-Nb composites, many works have focused on the strength or hardness, and the interface is considered as a vital factor on the properties [1,24,25]. Theoretically, the supersaturation of Nb into Cu could induce solid solution hardening as well as the lattice stresses, and the strength or hardness increases up to a level higher than that in the systems without solid solution. Since the solid solution is often neglected in most work due to the limited thermodynamics driving force, and thus, the solid solution has been so little coverage of the reports in ADB/ARB Cu-Nb composites. The effects of the solid solution on the microstructure, properties and the mechanism are still not understood well.

In the present paper, the interface density and the solid solution induced by the severe plastic deformation were examined and it will be shown how solid solution occurs during the deformation and affects the

* Corresponding authors.
E-mail addresses: ldeng@fzu.edu.cn (L. Deng), xhl@fzu.edu.cn (H. Xiang).

https://doi.org/10.1016/j.matchar.2019.02.002
Received 16 November 2018; Received in revised form 2 February 2019; Accepted 2 February 2019
Available online 05 February 2019
1044-5803/

microhardness.

2. Experimental methods

The studied Cu-16%Nb (vol. percentage) microcomposite wires were fabricated by accumulative drawing and bundling (ADB) process. The first stage is inserting a high pure Nb rod into an oxygen free high conductivity Cu tube, followed by series of hot extrusion, cold drawing and bundling cycles repeated 4 times. The processing details can be found in previous work [26,27]. The wires were subjected to accumulative strains (η) of 24.8, 26.0 and 26.4 respectively. The microstructure examination was carried out at a Zeiss Supra 55 scanning electron microscope (SEM) at an accelerating voltage of 15 kV. The SEM samples were etched in a solution of 20% nitric acid in 80% deionized water. The interface area density was determined from several cross sectional SEM images and the method has been illustrated in our previous work [12] and is also given in Appendix I. Meanwhile, the longitudinal section microstructure was examined by a JEM 2011 transmission electron microscope (TEM) operating at 200 kV. The TEM sample was prepared mechanical polishing followed by ion milling. X-ray diffraction (XRD) measurements were conducted on the longitudinal sections between 30° and 65° at room temperature by an X'pert3 diffractometer with a Cu target. 12 Vickers microhardness values were obtained for each sample on a THV-MDTe hardness machine with a 100 g load and a 10 s holding time. The averages were used for analyses.

3. Results and discussion

In our study, Nb changed in form after deformation from hexagonal rods to a ribbon shape [27]. In samples subjected to three levels of high strain, these ribbons remained straight and parallel to the axis direction (AD) when viewed in longitudinal direction. Viewed cross-sectionally, their curling morphology became evident, with no noticeable changes from one level to the next (Fig. 1). This curling morphology has been attributed not only to the deformation mechanism of Nb but also to the presence of Cu-Nb interfaces [27]. Curling with small radii of curvature manifests the presence of large elastic stresses [28].

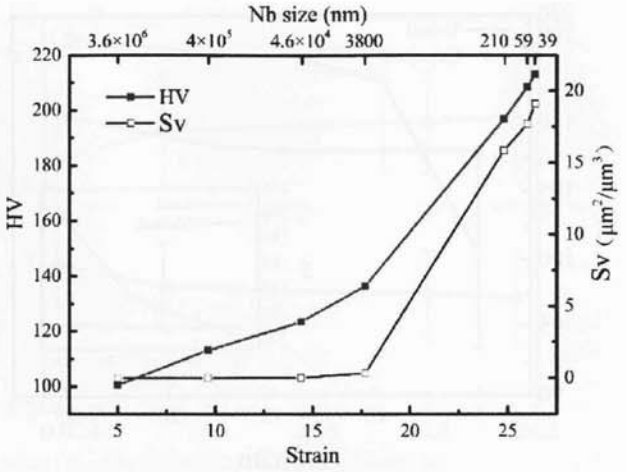

Fig. 2. Development of interface area density (Sv) and hardness (HV) at different strains. The data for samples with strains below 24.8 were obtained from our previous work [34].

The average thickness of Nb ribbons decreased from 210 nm at a strain of 24.8 to 59 nm at a strain of 26.0 and 39 nm at a strain of 26.4. We assumed that this decrement was accompanied by progressively more severe internal stress.

Interface area density, which plays a critical role in mechanical properties, can be attributed to changes in the curling of Nb ribbons [12,29,30]. It goes up as strain increases and Nb size (i.e. the average width of Nb ribbons) decreases. Likewise, hardness values increase as density increases and size decreases (Fig. 2). This indicates an obvious link between hardness and interface area density, in that both increase sharply when strain rises above 17.7. It is believed the materials with nanocrystals are significantly stronger than those with microscale grains [31]. In previous work, we found that interface area density increases markedly when Nb size is reduced to submicro or nano range [27]. In most nanostructured materials produced by severe plastic deformation where microstructure size has decreased to a few hundred

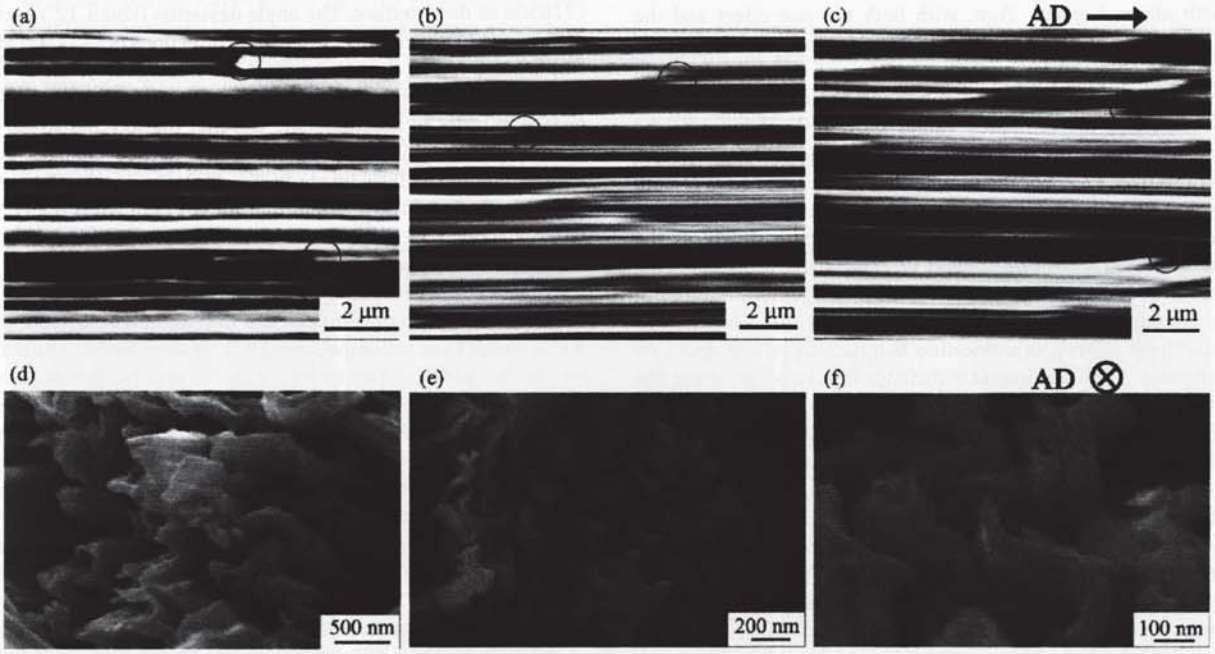

Fig. 1. Longitudinal section ((a)–(c)) and cross section ((d)–(f)) images: (a) and (d), η = 24.8; (b) and (e), η = 26.0; (c) and (f), η = 26.4. AD refers to axis direction. Some of the Nb ribbons were broken off due to ultrasonic vibration during sample cleaning, leaving behind Nb tips. In both cross sectional and longitudinal sectional images, the bright areas indicate Nb ribbons and the dark ones Cu matrix that has been removed during acid etching. Both the longitudinal and cross sectional morphology show little change as strain rises.

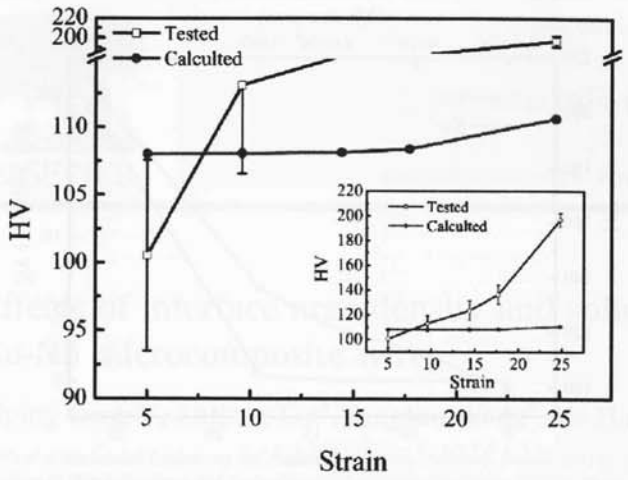

Fig. 3. Hardness evolution as a function of strains. The major figure shows the evolution with a broken HV range from 90 to 220, and the inset shows a full curve of the evolution. The black open diamonds are data from the experimental values and the red solid circles are data from calculations. (For interpretation of the references to colour in this figure legend, the reader is referred to the web version of this article.)

nanometers, the typical Frank-Read dislocation source may no longer exist [4]. In other words, submicro or nano sized Nb is probably not large enough for dislocations [32,33].Thus, decreased size induces sharp growth in HV values. Consequently, little or no dislocation accumulation should be observed inside Nb ribbons.

As stated above, the hardness in the present work changes significantly as the strain/*Sv* rises or the Nb size decreases. Our previous work indicated that the hardness of Cu-Nb composite wires is mainly dependent on and can be expressed by the Cu-Nb interface area density as well as the Nb size [12]. A model concerning interface density as the variable for modifying the H-P formula was proposed to evaluate the effect of microstructure dimensions on microhardness. The model predicted that the mirohardness increased with the interface density increasing. As far as this study is concerned, the model is effective although with allowed errors. Thus, with both the size effect and the interface area density being taken into consideration, the estimated hardness can be obtained for our wires, as the red curve displayed in Fig. 3. The black open diamond curve presents the experimental data. As can be seen that the estimated values show little changes as the strain increases. While, the tested data display obvious changes, especially at strains over 17.7. For the samples below 17.7, the sizes of both Cu matrix and Nb ribbons are quite beyond nano range (above 3.8 μm [34]); the Cu-Nb interface density is expected to rise slowly as the strains increases [12]. For those beyond 17.7, the sizes reach nanoscale where size effect becomes significant; on the other hand, the interface density grow quickly with increasing strains, and the interface-dislocation reactions, pinning of dislocation at interfaces as well as single dislocation propagation for interface distance dominate, resulting the noticeably increment of mirohardness [35]. It is to be noted that the estimated values don't match well with the tested values, especially for those at strains above 10. For these wires, the tested values are higher than the estimated ones, and the higher the strains, the more the deviation. It's also worth noting that the estimation is only reasonable for the wires with low strains where the strengthening effect mainly consists of work hardening and size-effect hardening. While, in the present work, the wires underwent strains up to 24.8, which is much higher than those in the Ref [12]. This differences are so striking that other strengthening mechanism, such as solid solution effect, is suggested to be taken into account.

Fig. 4 shows the XRD patterns of the samples with different strains. Both Cu and Nb peaks can be observed and the three patterns show clear differences. In Fig. 4(a) the Cu peaks shift toward lower diffraction angle as the strain goes up while the Nb peaks toward higher angles. This peak shifts to lower angle correspond to an increase of the lattice parameter of Cu matrix and that to higher angle corresponds to a decrease of the lattice parameter of Nb ribbons. These changes in lattice parameters of both Cu and Nb are also shown in Fig. 4(b) where the lattice constant of Cu increases with the increment of strains and that of Nb decreases. Besides, it is shown in Fig. 4(a) that the deformation broadens the XRD peaks due to the refinement of the grains and the introduction of lattice strain [36]. These two factors induce the lattice constants to dev0iate from the standard ones, which is mainly attributed to the severe plastic deformation, the solid solution [37,38] and lattice distortion [39,40]. The more the deformation, the more the lattice constant changes or lattice distortion and then the more the peak shifts. In addition, the solid solution hardening and the lattice distortion are suggested to associate with the supersaturation of Nb into Cu matrix, and this is believed to contribute the high strength of Cu-Nb [36].

For better observation of the lattice distortion and solid solution, TEM as well as high resolution transmission electron microscopy (HRTEM) technologies were applied on the sample with a strain of 24.8, and the results are shown in Fig. 5. Low magnification TEM image (Fig. 5(a)) shows Nb ribbons and Cu matrix in ribbon shapes with a width of about 50–150 nm in alternant arrangement. The inset is the selected area electron diffraction pattern showing a quite parallel relationship of ⟨011⟩Nb and ⟨111⟩Cu. Fig. 5(b) shows one HRTEM image resolving the atomic structure between Cu and Nb grains as well as the interface. The corresponding fast Fourier transform (FFT) patterns are inserted, in which (111) and (002) type reflections for the [110]Cu incident beam and (011) type reflection for the [111]Nb incident beam were observed. This implies a typical Kurdjumov-Sachs relationship ({111}⟨110⟩Cu//{110}⟨111⟩Nb) between Cu matrix and Nb ribbon. Fig. 5(c) is an inverse fast Fourier transformation (IFFT) image showing the structure of the rectangle region in Fig. 5(b) and resolving the Cu-Nb interface microstructure. It can be seen that the interface (shown by the dashed lines in Fig. 5(c)) is somewhat disordered region in ~2–3 nm wide which may be due to the fact that the interface is not strict edge-on. This apparent interface separates the Cu matrix and Nb ribbons with a typical Kurdjumov-Sachs relationship of {110}⟨111⟩Nb//{111}⟨110⟩Cu at the interface. The angle deviation (about 12°) between the planes of (111)Cu and (011)Nb (or the directions of ⟨111⟩Cu and ⟨011⟩Nb) is much higher than that (about 1.8°) in Fig. 5(a), which is so large that it would induce a significant distortion of lattice around the interface in order to accommodate or relief the internal stress. This has been confirmed by the peak shifts and lattice changes in Fig. 4. Meanwhile, in the IFFT image in Fig. 5(c), the spacing between (111) planes in Cu is 0.2168 nm, and that for (011) in Nb is 0.2447 nm. The latter is about 1.13 times the former. While, for an ideal structure, the ratio of the interplanar spacing of (011)Nb over (111)Cu is 1.12. This discrepancy is expected for this submicro structure and indicates that, in [111]Cu, the internal stresses are in tension and in [011]Nb the internal stresses are in compression [40]. In some region of the interface, e.g. in the white ellipse in Fig. 5(c), Cu and Nb lattices seem to be overlapped because of the inclined interface with respect to the beam. It seems that the defect storage occurs at the interface and the co-deformation between Cu and Nb may induce distortion between these two phases. After severe plastic deformation, the Cu-Nb interfaces are expected to be semi-coherent with a few misfit dislocations [7]. In our sample, several misfit dislocations (⊥ symbols) near Cu side can be observed, as shown in Fig. 5(c). While, in Nb ribbons, there is no dislocation observed. This is mainly due to the slip discontinuity and the lattice misfit between Cu and Nb, and the small size of Nb ribbons in the samples These cause the dislocation transmission across the Cu-Nb interfaces to be particularly difficult [4,32,33]. Meanwhile, the glide of dislocations in Cu toward the interface is more energetically favorable than that for the case of the dislocations in Nb, and dislocation transmission from Cu to Nb has not been found even at a high enough strain

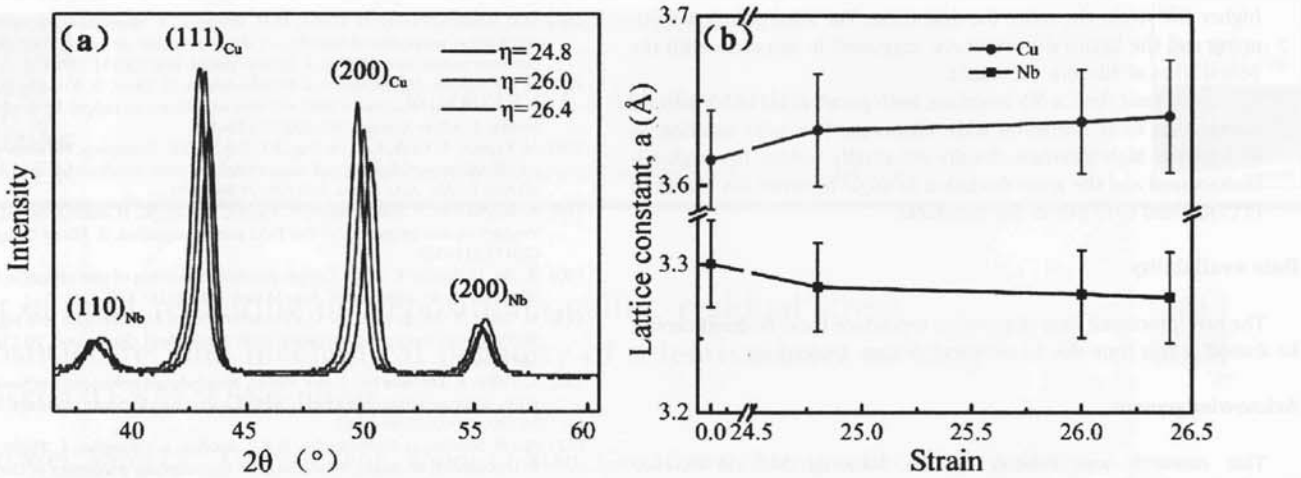

Fig. 4. XRD data. (a) XRD patterns of the wires with different levels of strain at 24.8, 26.0 and 26.4; (b) development of lattice constants of Cu matrix and Nb ribbons under different strains.

[32]. Thus, more dislocations pile up in the interfaces nearby the Cu matrix.

Around the interface, some regions with disordered crystallographic lattice structure can be observed. Examples are shown by the white rectangle and the circle in Fig. 5(c). This is suggested to be the regions where Nb atoms dissolved into Cu matrix during the severe plastic deformation. Near this region, a small area with atoms arranging differently can be observed, as marked by the red tetragon *I* in the top-left corner. This distorted region extends to distances larger than those regions (red tetragon areas *II* and *III*) expected from a local distortion caused by a single misfit dislocation [39]. It stands a good chance that the distortion can results in dissolution of Nb in Cu. Goog et al. [41] and Raabe et al. [42] have reported that the solution between Cu and Nb took place when the phases underwent deformation-induced mixing although with the absence of thermodynamics driving force, and the solubility was found to be far beyond the equilibrium. They also proposed the trans-phase dislocation-shuffling mechanism for the mixing of Cu and Nb phases. During severe plastic flow the lattice dislocations penetrate the interfaces nearby Cu phase, promoting certain atoms into the neighboring phase and misfit dislocations into the interface, leaving the chemical mixing as well as the disordered and distorted regions as the red tetragon area *I* shown in Fig. 5(c). Attributed to the disordered interface developed by plastic deformation and the fact that the dislocation movement occurs on essentially every lattice plane, those dislocations deriving from Cu would store predominantly around or at the interface rather than penetrate the interface to Nb ribbons [32,43–45]. On the other hand, the slip discontinuity introduces dislocation transmission particularly difficult [32] and results in dislocations storing around the interface as well as more atoms pushed into the interfaces, leaving the disordered, wide and blurred interface. Both the interfaces, and these disordered and distorted regions induced by solid solution are believed to be able to effectively hinder the dislocation slip, making a contribution to the mircohardness.

4. Conclusions

Both the microstructure and the microhardness of the ADB Cu-Nb wires show changes as a function of the strains. The interface area density as well as the solid solution effect was suggested to account for the changing of microhardness. The main results can be drawn as follows:

(1) The interface area density and the microhardness increase with almost the same trend as the strain increases. While, the estimated microhardness values show much lower than the tested ones when the samples subjected to high strains. Solid solution effect is suggested for the discrepancy.
(2) The XRD results imply lattice distortion in all the samples and the

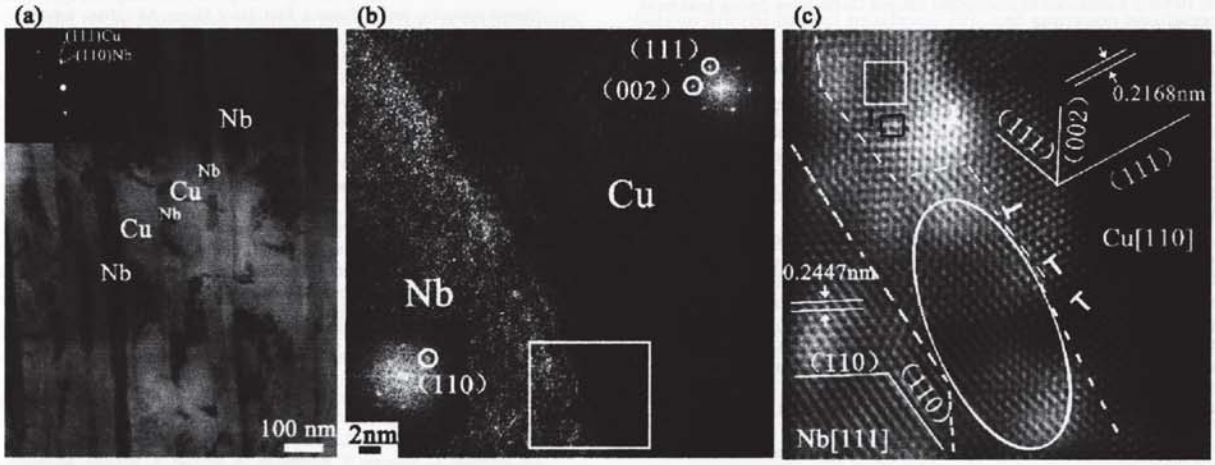

Fig. 5. TEM and HRTEM images of Cu-Nb microcomposites at a strain of 24.8. (a) bright field image with the selected area electron diffraction pattern; (b) HTREM image with corresponding FFT patterns of both Cu matrix and Nb ribbons; (c) inverse fast Fourier transformation (IFFT) image corresponding to the rectangle region in Fig. 5(b); the approximate interface positions are indicated by white broken lines.

higher the strain the more the distortion. The solid solution hardening and the lattice distortion are suggested to associate with the penetration of Nb into Cu matrix.

(3) In regions near the Cu-Nb interface, both penetration of Nb into Cu matrix and local distortion were observed. The solid solution as well as the high interface density essentially induce the high microhardness and the great deviation in angle between the planes of (111)Cu and (011)Nb at the interfaces.

Data availability

The raw/processed data required to reproduce these findings cannot be shared at this time due to technical or time limitations.

Acknowledgement

This research was funded by the National Natural Science Foundation of China (No. 51601039), the Natural Science Foundation of Fujian Province of China (No. 2016J05119), Major special project of Fujian Science and Technology Program (No. 2017HZ0001-2), and Fuzhou University Testing Fund of precious apparatus (No. 2018T018). A portion of this work was also supported by the National High Magnetic Field Laboratory through US National Science Foundation Cooperative Agreement (No. DMR-1157490) and Fujian Provincial Collaborative Innovation Center for High-end Equipment Manufacturing. We thank Dr. Tyler for editing the manuscript.

Appendix A. Supplementary data

Supplementary data to this article can be found online at https://doi.org/10.1016/j.matchar.2019.02.002.

References

[1] C.J. Schneider Judy, S. Carpenter John, A. Mara Nathan, Maintaining nano-lamellar microstructure in friction stir welding (FSW) of accumulative roll bonded (ARB) Cu-Nb nano-lamellar composites (NLC), J. Mater. Sci. Technol. 34 (1) (2018) 92–101.
[2] L. Ghalandari, M.M. Mahdavian, M. Reihanian, Microstructure evolution and mechanical properties of Cu/Zn multilayer processed by accumulative roll bonding (ARB), Mater. Sci. Eng. A 593 (Supplement C) (2014) 145–152.
[3] F. Heringhaus, D. Raabe, G. Gottstein, On the correlation of microstructure and electromagnetic properties of heavily cold worked Cu-20%wt% Nb wires, Acta Metall. Mater. 43 (4) (1995) 1467–1476.
[4] M.R. Toroghinejad, R. Jamaati, J. Dutkiewicz, J.A. Szpunar, Investigation of nanostructured aluminum/copper composite produced by accumulative roll bonding and folding process, Mater. Des. 51 (2013) 274–279.
[5] L. Deng, K. Han, B. Wang, X. Yang, Q. Liu, Thermal stability of Cu–Nb microcomposite wires, Acta Mater. 101 (2015) 181–188.
[6] R. Lei, M. Wang, S. Xu, H. Wang, G. Chen, Microstructure, hardness evolution, and thermal stability mechanism of mechanical alloyed Cu-Nb alloy during heat treatment, Metal 6 (9) (2016) 194.
[7] F. Dupouy, E. Snoeck, M.J. Casanove, C. Roucau, J.P. Peyrade, S. Askenazy, Microstructure characterization of high strength and high conductivity nanocomposite wires, Scr. Mater. 34 (7) (1995) 1067–1073.
[8] T. Gu, J.R. Medy, F. Volpi, O. Castelnau, S. Forest, E. Hervé-Luanco, F. Lecouturier, H. Proudhon, P.O. Renault, L. Thilly, Multiscale modeling of the anisotropic electrical conductivity of architectured and nanostructured Cu-Nb composite wires and experimental comparison, Acta Mater. 141 (Supplement C) (2017) 131–141.
[9] U. Saikia, M.B. Sahariah, R. Pandey, Stability of Cu–Nb layered nanocomposite from chemical bonding, Chem. Phys. Lett. 655–656 (2016) 59–65.
[10] X. Xu, Y. Lu, M. Liang, Z. Liu, F. Zhang, C. Li, Heat treatment effect on the magnetic properties of Cu-Nb micro-composites, IEEE Trans. Appl. Supercond. 22 (3) (2012).
[11] R.N. Jabdaraghi, J.T. Peltonen, O.-P. Saira, J.P. Pekola, Low-temperature characterization of Nb-Cu-Nb weak links with Ar ion-cleaned interfaces, Appl. Phys. Lett. 108 (4) (2016) 042604.
[12] L. Deng, K. Han, K.T. Hartwig, T.M. Siegrist, L. Dong, Z. Sun, X. Yang, Q. Liu, Hardness, electrical resistivity, and modeling of in situ Cu–Nb microcomposites, J. Alloys Compd. 602 (0) (2014) 331–338.
[13] H.I. Aaronson, A. John K, N.R. Adsit, S.M. Allen, P. Ambalal, R.J. Barnhurst, ASM Metal Handbook, ASM international, 1992.
[14] C. Suryanarayana, Mechanical alloying and milling, Prog. Mater. Sci. 46 (1–2) (2001) 1–184.
[15] S. Mula, H. Bahmanpour, S. Mal, P.C. Kang, M. Atwater, W. Jian, R.O. Scattergood, C.C. Koch, Thermodynamic feasibility of solid solubility extension of Nb in Cu and their thermal stability, Mater. Sci. Eng. A 539 (2012) 330–336.
[16] M.D. Abad, S. Parker, D. Kiener, M.M. Primorac, P. Hosemann, Microstructure and mechanical properties of CuxNb1 – x alloys prepared by ball milling and high pressure torsion compacting, J. Alloys Compd. 630 (2015) 117–125.
[17] E. Botcharova, M. Heilmaier, J. Freudenberger, G. Drew, D. Kudashow, U. Martin, L. Schultz, Supersaturated solid solution of niobium in copper by mechanical alloying, J. Alloys Compd. 351 (2003) 119–125.
[18] M. Kapoor, T. Kaub, K.A. Darling, B.L. Boyce, G.B. Thompson, An atom probe study on Nb solute partitioning and nanocrystalline grain stabilization in mechanically alloyed Cu-Nb, Acta Mater. 126 (2017) 564–575.
[19] A. Moghanian, F. Sharifianjazi, P. Abachi, E. Sadeghi, H. Jafarikhorami, A. Sedghi, Production and properties of Cu/TiO2 nano-composites, J. Alloys Compd. 698 (2017) 518–524.
[20] N. Jia, D. Raabe, X. Zhao, Crystal plasticity modeling of size effects in rolled multilayered Cu-Nb composites, Acta Mater. 111 (2016) 116–128.
[21] M. Liang, Y. Lu, Z. Chen, C. Li, Characteristics of high strength and high conductivity Cu-Nb micro-composties, IEEE Trans. Appl. Supercond. 20 (3) (2010) 1619–1621.
[22] L. Thilly, F. Lecouturier, J. von Stebut, Size-induced enhanced mechanical properties of nanocomposite copper/niobium wires: nanoindentation study, Acta Mater. 50 (20) (2002) 5049–5065.
[23] M.J.R. Sandim, D. Stamopoulos, H.R.Z. Sandim, L. Ghivelder, L. Thilly, V. Vidal, F. Lecouturier, D. Raabe, Size effects on the magnetic properties of Cu-Nb nanofilamentary wires processed by severe plastic deformation, Supercond. Sci. Technol. 19 (12) (2006) 1233–1239.
[24] J.B. Dubois, L. Thilly, F. Lecouturier, P. Olier, P.O. Renault, Cu/Nb nanocomposite wires processed by severe plastic deformation for applications in high pulsed magnets: effects of the multi-scale microstructure on the mechanical properties, IEEE Trans. Appl. Supercond. 22 (3) (2012) 6900104/1–6900104/4.
[25] N.A. Mara, D. Bhattacharyya, R.G. Hoagland, A. Misra, Tensile behavior of 40 nm Cu/Nb nanoscale multilayers, Scr. Mater. 58 (2008) 874–877.
[26] L. Ming, Study on Fabrication and Properties of CuNb(Sn) Materials for High Field Magnet, Northwestern Polytechnical University, 2010.
[27] L. Deng, X. Yang, K. Han, Y. Lu, M. Liang, Q. Liu, Microstructure and texture evolution of Cu–Nb composite wires, Mater. Charact. 81 (2013) 124–133.
[28] S.I. Hong, M.A. Hill, Y. Sakai, J.T. Wood, J.D. Embury, On the stability of cold drawn, two-phase wires, Acta Metall. Mater. 43 (9) (1995) 3313–3323.
[29] I.L. Deryagina, E.N. Popova, E.G. Valova-Zaharevskaya, E.I. Patrakov, Structure and thermal stability of high-strength Cu–18Nb composite depending on the degree of deformation, Phys. Met. Metallogr. 119 (1) (2018) 92–102.
[30] A. Nye, A.C. Leff, C.M. Barr, M.L. Taheri, Direct observation of recrystallization mechanisms during annealing of Cu in low and high strain conditions, Scr. Mater. 146 (2018) 308–311.
[31] J.R. Weertman, Hall-Petch strengthening in nanocrystalline metals, Mater. Sci. Eng. A 166 (1) (1993) 161–167.
[32] J. Wang, R.G. Hoagland, J.P. Hirth, A. Misra, Atomistic modeling of the interaction of glide dislocations with "weak" interfaces, Acta Mater. 56 (19) (2008) 5685–5693.
[33] N. Wang, Microstructures and mechanical properties of nanocrystlline materials, Metallurgy and Materials Science, University of Toronto, Ottawa, 1997, p. 205.
[34] L. Deng, X. Yang, K. Han, Z. Sun, Q. Liu, Study of the microstructure evolution of Cu-Nb composite wires during deformation and annealing, Acta Metall. Sin. 50 (2) (2014) 231–237.
[35] R.F. Zhang, T.C. Germann, J. Wang, X.Y. Liu, Role of interface structure on the plastic response of Cu/Nb nanolaminates under shock compression, Scr. Mater. 68 (2013) 114–117.
[36] K.M. Youssef, M.A. Abaza, R.O. Scattergood, C.C. Koch, High strength, ductility, and electrical conductivity of in-situ consolidated nanocrystalline Cu-1%Nb, Mater. Sci. Eng. A 711 (2018) 350–355.
[37] J.-K. Lee, S.-Y. Kim, R.T. Ott, J.-Y. Kim, J. Eckert, M.-H. Lee, Effect of reinforcement phase on the mechanical property of tungsten nanocomposite synthesized by spark plasma sintering, Int. J. Refract. Met. Hard Mater. 54 (2016) 14–18.
[38] J. Eckert, A. Kubler, L. Schultz, Mechanically alloyed Zr55Al10Cu30Ni5 metallic glass composites containing nanocrystalline W particles, J. Appl. Phys. 85 (10) (1999) 7112–7119.
[39] K. Han, K.Y. Zhang, H. Kung, J.D. Embury, B.J. Daniels, B.M. Clemens, A structure investigation of epitaxial Fe-Pt multilayers, Philos. Mag. A 82 (8) (2002) 1633–1650.
[40] T.D. Shen, X. Zhang, K. Han, C.A. Davy, D. Aujla, P.N. Kalu, R.B. Schwarz, Structure and properties of bulk nanostructured alloys synthesized by flux-melting, J. Mater. Sci. 42 (2007) 1638–1648.
[41] H.R. Gong, B.X. Liu, Unusual alloying behavior at the equilibrium immiscible Cu-Nb interfaces, J. Appl. Phys. 96 (5) (2004) 3020–3022.
[42] D. Raabe, S. Ohsaki, K. Hono, Mechanical alloying and amorphization in Cu-Nb-Ag in situ composite wires studied by transmission electron microscopy and atom probe tomography, Acta Mater. 57 (17) (2009) 5254–5263.
[43] J. Wang, R.G. Hoagland, J.P. Hirth, A. Misra, Atomistic simulations of the shear strength and sliding mechanisms of copper–niobium interfaces, Acta Mater. 56 (2008) (2008) 3109–3119.
[44] J.D. Embury, C.W. Sinclair, The mechanical properties of fine-scale two-phase materials, Mater. Sci. Eng. A 319 (2001) 37–45.
[45] E. Snoeck, F. Lecouturier, L. Thilly, M.J. Casanove, H. Rakoto, G. Coffe, S. Askenazy, J.P. Peyrade, C. Roucau, V. Pantsyrny, A. Shikov, A. Nikulin, Microstructural studies of in situ produced filamentary Cu/Nb wires, Scr. Mater. 38 (11) (1998) 1643–1648.